Received 21 February, 2022; revised 16 March, 2022; accepted 25 May, 2022. Date of publication 30 May 2022; date of current version 8 June 2022.
The review of this article was arranged by Editor S. Vaziri.

*Digital Object Identifier 10.1109/JEDS.2022.3178742*

# High-Performance Field Electron Emitters Fabricated Using a Free-Standing Carbon Nanotube Film

**JUN SOO HAN, SANG HEON LEE, AND CHEOL JIN LEE**

School of Electrical Engineering, Korea University, Seoul 02841, Republic of Korea

CORRESPONDING AUTHOR: CHEOL JIN LEE (e-mail: cjlee@korea.ac.kr)

This work was supported in part by the National Research Foundation of Korea's Brain Korea 21 FOUR Program and in part by the National Research Foundation of Korea (NRF) Grant funded by the Korea Government (MSIT) under Grant NRF-2019R1A2C2010267.

**ABSTRACT** The carbon nanotube (CNT) field emitter was fabricated using a thin free-standing CNT film, indicating a line-shape CNT field emitter. Field emission properties of the CNT field emitter were investigated in both diode and triode configurations. The CNT field emitter showed a low turn-on electric field of 1.8 V/μm and a high emission current of 40.3 mA, corresponding to the emission current density of 96 A/cm$^2$ in the diode configuration. It also exhibited a high anode current of 40 mA, corresponding to the anode current density of 95.2 A/cm$^2$ in the triode configuration. In addition, the CNT field emitter showed a good electron beam transmittance of 86.4% and excellent emission stability without degradation for 15 h. The main reason for the high performance of our CNT field emitter is caused by the high density of emission sites at the edge of the CNT film.

**INDEX TERMS** Carbon nanotube (CNT), field emission, field emitter, Carbon nanotube film.

## I. INTRODUCTION

Carbon nanotubes (CNTs) have attracted attention as promising field emission materials due to their excellent electrical and thermal conductivity, good mechanical strength, stable chemical endurance, and high aspect ratio [1]–[4]. CNT field emitters have been studied to obtain high emission current and good emission stability for several applications to electron beam sources, lamps, microwave amplifiers, and X-ray sources [5]–[9]. CNT field emitters have previously been fabricated using various methods: (i) an as-grown CNTs [10]–[12], (ii) electrophoresis attached CNTs [13], [14], (iii) a CNT paste using organic binder [15]–[19], and (iv) a CNT yarn [20], [21]. CNT paste emitters have been mainly used because they showed good mechanical adhesion between the CNT paste and the cathode substrate and indicated a relatively high emission current density [18], [19]. However, organic binder material which is used to fabricate a CNT paste often makes a drawback of CNT paste emitters due to outgassing originated by the residue of organic binder [22], [23]. The key to realizing high-performance CNT field emitters is to increase both the emission current and the emission current density by increasing the emission site density, and also guarantee good emission stability by reducing outgassing. In this work, we suggest a unique CNT field emitter made by a free-standing CNT film. The proposed CNT field emitter uses a cross-section of the free-standing CNT film as an emission site. It is fabricated using a simple method that clamps the CNT film with metal plates [24]. As an organic material is not used to fabricate the CNT field emitter, there is almost no outgassing. As a result, stable electron emission is induced. Our CNT field emitter shows extremely high emission current density and also indicates a good emission stability.

## II. EXPERIMENTAL DETAILS

Fig. 1(a) shows schematics of the fabrication method of the CNT field emitter with a line-shape using a free-standing CNT film. The free-standing CNT film was fabricated using single-walled CNTs (SWCNTs). SWCNTs were produced by an arc discharge method, and the $I_G/I_D$ ratio of the SWCNTs

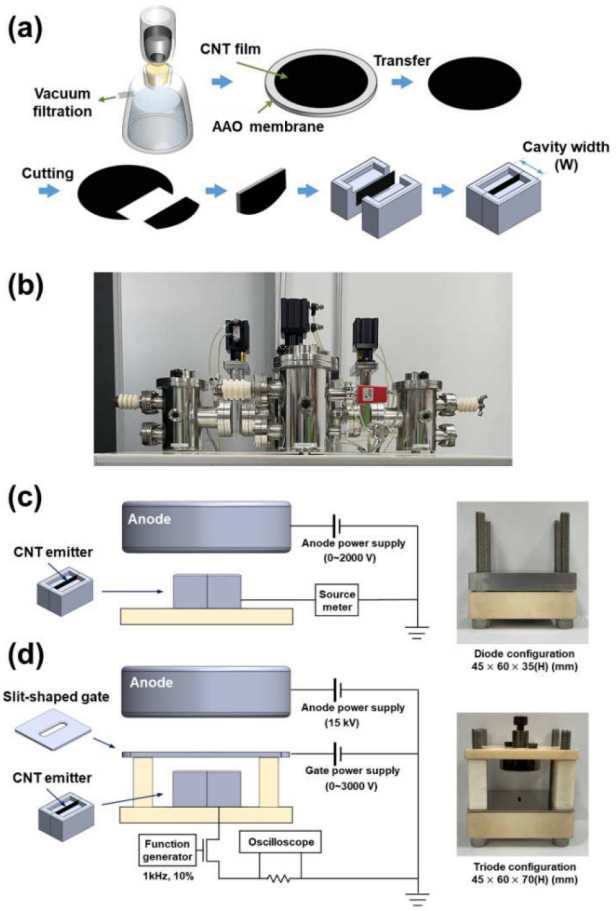


**FIGURE 1. (a) Schematics of fabrication method of the CNT field emitter with a line-shape using free-standing CNT film. (b) Vacuum chamber used for field emission. The field emission measurement in the diode configuration (c) and triode configuration (d).**

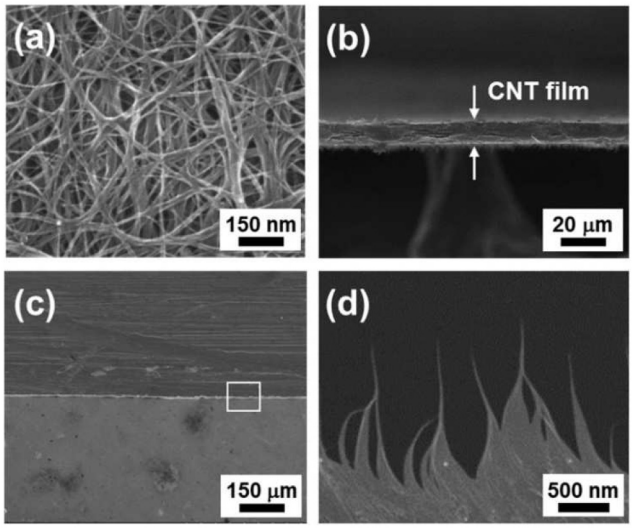


**FIGURE 2. (a) SEM image of surface morphology of CNT film. (b) SEM image of top view of the edge of CNT film. (c) SEM image of the side view of the edge of CNT film. (d) SEM image of tips of CNT bundles at the edge of CNT film.**

was 48, indicating very high crystallinity without any defects. The SWCNT powder was added to a 0.1 wt% sodium dodecyl sulfate solution and dispersed using the ultrasonication method. The dispersed solution was filtered through anodic aluminum oxide (AAO) membrane using a vacuum filtration method and a free-standing CNT film was produced by eliminating the AAO membrane [25]. The CNT film became completely dense and had high purities through the post-treatment process. After cutting the free-standing film into a uniform rectangular shape using a razor, the stainless steel metal plates were clamped from both sides of the film to fix it firmly. The height and height uniformity of the inserted CNT film were controlled using a supporting jig. The CNT film and the metal plate had a contact surface of 1 mm in three directions (left, right, and bottom). The contact resistance between the CNT film and the metal plate was 0.22 Ω with a contact area of 10 $mm^2$. The cathode electrode has a cavity with a depth of 1 mm to enable the uniform distribution of the electric field in the length direction. Fig. 1(b) shows an optical photo image of vacuum chamber used for the field emission measurement. The field emission characteristics of the CNT field emitters were measured in a vacuum pressure of $\sim 9 \times 10^{-8}$ Torr. Fig. 1 (c) shows schematics of the field emission measurements in a diode configuration. The diode configuration consisted of a SUS304 anode and cathode. The CNT field emitter had a thickness of 7 μm and a length of 6 mm. The gap between the two electrodes was set to 0.5 mm. The anode voltage was applied using a voltage source (TECHNIX SR15-P-1500). The emission current was measured using a source meter (Keithley 2400) in a direct current (DC) operating mode. Fig. 1(d) shows schematics of the field emission measurements in a triode configuration. The triode configuration consisted of a SUS304 anode, slit-shape gate, and cathode electrodes. A gate electrode with a slit-shaped hole was inserted between the anode and cathode electrodes. The slit of the gate electrode has a width and length of 1.5 mm and 6 mm respectively. The gap between the anode and gate electrodes was set to 20 mm, and the gap between the gate and cathode electrodes was set to 0.5 mm. The field emission characteristics were measured in the pulse operating mode with a frequency of 1 kHz and duty of 10%. A constant voltage of 15 kV was applied to the anode electrode using a high voltage source (Spellman SL1200) with the measurement of the anode current. The emission current was measured using an oscilloscope (Tektronix TDS2012C) and the gate leakage current was measured using a source meter (Keithley 2290). The field emission pattern was obtained using phosphor-coated indium tin oxide (ITO) glass as an anode electrode under the same conditions.

## III. RESULTS AND DISCUSSION

Fig. 2(a) shows an SEM image of the surface morphology of the CNT film. The morphology of the CNT film was analyzed using scanning electron microscopy (SEM) (Hitachi

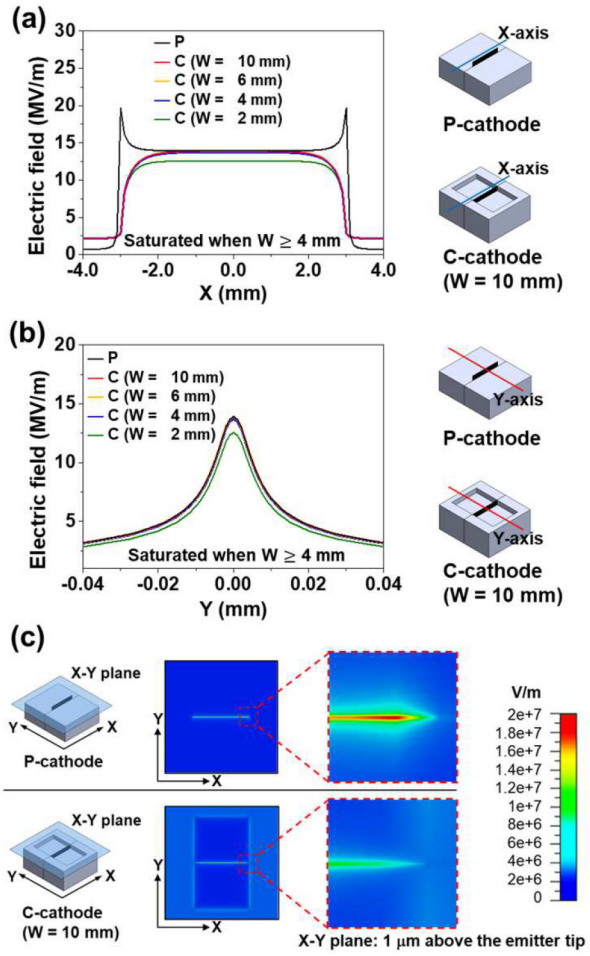


**FIGURE 3. Simulation of the cathode electrode structure for the CNT field emitter. (a) The electric field distribution along the length direction (x-axis) of the film. (b) The electric field distribution along the thickness direction (y-axis) of the film. (c) The top-view electric field distribution in the x-y plane.**

S-4800). The CNTs are tightly entangled by van der Waals force and form a high density CNT network without impurities. Fig. 2(b) shows an SEM image of the top view of the edge of the CNT film, which indicates the cross-section of the film. The CNT film has a uniform thickness of 7 μm over the entire length. Fig. 2(c) shows an SEM image of the side view of the edge of the free-standing CNT film after razor cutting. Fig. 2(d) shows a high-magnification SEM image of tips of CNT bundles in the white box of Fig. 2(c) which indicates that several SWCNT bundles are aligned in the upward direction, which is favorable for electron emission properties. The simulation results for the electric field distribution of the CNT field emitter with a length of 6 mm, which is dependent on the structure of the cathode electrode are shown in Fig. 3(a)∼(c). All simulation results were obtained in a diode configuration using the CST Studio program. The gap between the cathode and the anode electrodes was set to 0.5 mm, and a voltage of 1000 V was applied to the anode electrode. The electric field distribution simulation was performed 1 μm above the tip of the CNT field emitter. The emission sites were set uniformly in the cross-section of the CNT film, and the Fowler–Nordheim equation was used to evaluate the field emission characteristics of each emission site of the SWCNTs. Fig. 3(a) shows simulation results of the electric field distribution of the CNT field emitter along the length direction (x-axis) of the CNT film. A planar-type cathode electrode (P-cathode) was produced by clamping a rectangular CNT film with two flat metal plates. It shows a sharply increased electric field distribution at both ends of the CNT film, which is caused by an excessively concentrated electric field at the end of the protruding CNT film. On the other hand, the cavity-type cathode electrode (C-cathode) was produced by clamping a rectangular CNT film with two cavity-shaped metal plates. The CNT field emitter with the C-cathode exhibited a uniform electric field distribution over the entire length of the CNT film because of effective suppression of the electric field at the end of the CNT film. The electric field was saturated to a level similar to that of the P-cathode when the width of the C-cathode was greater than 4 mm. Fig. 3(b) shows simulation results of the electric field distribution of the CNT field emitter along the thickness direction (y-axis) of the CNT film. The electric field is concentrated at the CNT film regardless of the cathode type, and the electric field is also saturated to a level similar to that of the P-cathode when the cavity width of the C-cathode is more than 4 mm. Fig. 3(c) shows simulation results of the top-view electric field distribution of the CNT field emitter. The electric field distribution is illustrated as a colormap of the x-y plane. For the P-cathode, the electric field is highly concentrated at the end of the CNT film as shown in the magnified image. On the other hand, for the C-cathode, the electric field was uniformly distributed throughout the CNT film. Fig. 4(a) shows the emission current (I) versus the applied electric field ($E_a$) curve of the CNT field emitter in the diode configuration. The turn-on electric field at the emission current density of 0.1 mA/cm$^2$ is 1.8 V/μm, and the threshold electric field at the emission current density of 1 A/cm$^2$ is 2.5 V/μm. The maximum emission current is 40.3 mA in an electric field of 3.8 V/μm, which corresponds to the maximum emission current density of 96 A/cm$^2$. In general, it is difficult to obtain both a high emission current and a high emission current density simultaneously because of the screening effect [26], [27]. However, the CNT field emitter exhibits both a high emission current and a high emission current density. This is caused by the high density emission sites of approximately 1.9 × 10$^6$ ea/cm$^2$ at the edge of the CNT film, which is calculated by an emission current obtained at the emission area. As a result, the CNT field emitter shows much better emission performance than the other CNT paste field emitters [16], [19], [28], [29]. The inset of Fig. 4(a) shows the Fowler-Nordheim (F-N) plot derived from the I-$E_a$ curve. Nonlinearity in the slope of the F-N plot is attributed to the conduction band current saturation of semiconducting characteristics of SWCNT at the high electric field [30]. The linear curve (red color) in the low

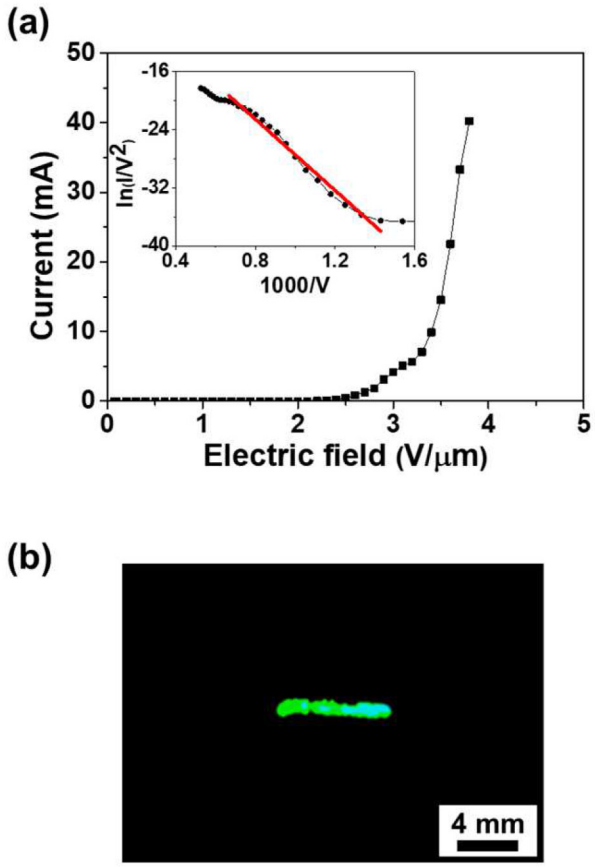


**FIGURE 4.** Field emission characteristics of the 6 mm CNT field emitter in the diode configuration. (a) I-$E_a$ characteristics of the CNT field emitter. The inset shows the F-N plot derived from the I-$E_a$ curve. (b) Electron emission pattern of the CNT field emitter (6.0 mm × 0.8 mm).

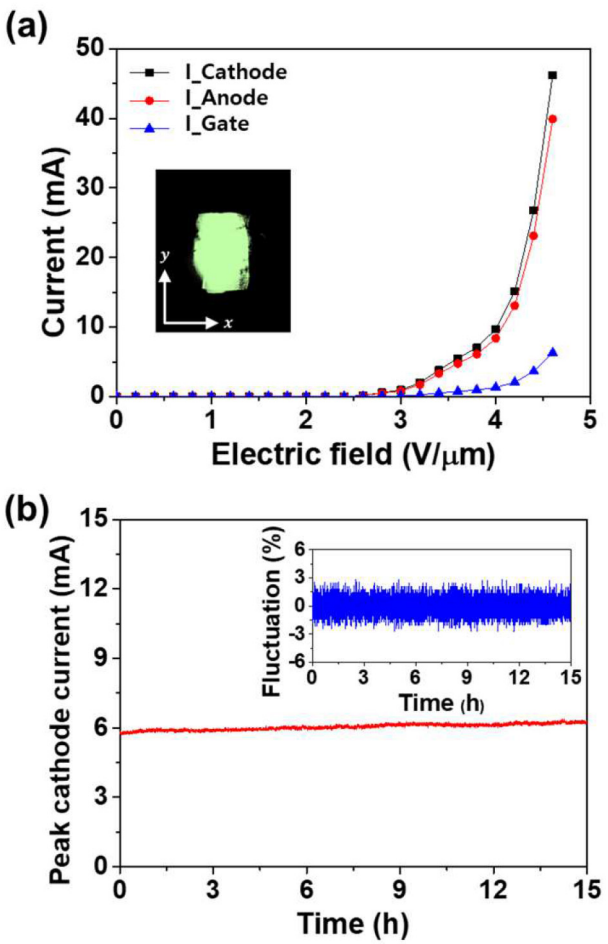


**FIGURE 5.** Field emission characteristics of the 6 mm CNT field emitter in the triode configuration. (a) I-$E_a$ characteristics of the CNT field emitter. The inset shows the electron emission pattern of the CNT field emitter (10.0 mm × 14.9 mm) (b) Long-term emission stability of the CNT field emitter. The inset shows the fluctuation of the emission current.

electric field region reveals the quantum tunneling behavior. For the CNT work function is 5 eV [31], the field enhancement factor ($\beta$) was evaluated to be 1561. Fig. 4(b) shows the emission pattern of the CNT field emitter in a diode configuration. In this work, an ITO glass coated with phosphor was used as the anode electrode. The gap between the anode electrode and the emitter was 0.5 mm, and the emission pattern was obtained at an emission current of 1 mA. The emission pattern (6 mm × 0.8 mm) reveals that the electron beam is evenly emitted from the entire edge of the CNT film with a length of 6 mm. Fig. 5(a) shows the emission current (I) versus the applied electric field ($E_a$) curve of the CNT field emitter in the triode configuration. The cavity width of the C-cathode was 4 mm, and the slit of the gate electrode had a width of 1.5 mm and a length of 6 mm. The gap between the anode and gate electrodes was 20 mm, and the gap between the gate and cathode electrodes was set to 0.5 mm. In the triode configuration, the field emission characteristics were measured in the pulse operating mode with a frequency of 1 kHz and 10% duty to minimize the heat accumulation phenomenon at the gate electrode during the field emission operation. The maximum anode current was 40 mA at a gate voltage of 2.3 kV, corresponding to the maximum anode current density of 95.2 A/cm$^2$. The obtained emission properties are much higher than those of other CNT paste field emitters [32]–[39]. As mentioned in the field emission characteristics of the diode configuration, both the high emission current and the high emission current density are attributed to the high density of emission sites at the edge of the CNT film. In addition, the electron beam transmittance through the gate electrode was calculated to be 86.4% at an anode voltage of 15 kV, which indicates a low gate leakage current. This means that the proposed gate electrode with a slit-shaped hole is appropriate for line-shape CNT field emitters. Interestingly, the threshold electric field of the CNT field emitter in the triode configuration is 2.7 V/μm. Compared to the diode configuration, the threshold electric field in the triode configuration marginally increased. This is attributed to a slightly reduced electric field owing to the hole of the gate electrode. The inset of Fig. 5(a) shows the electron emission pattern of the CNT field emitter in a triode configuration. The emission pattern was obtained at an emission current of 1 mA. The

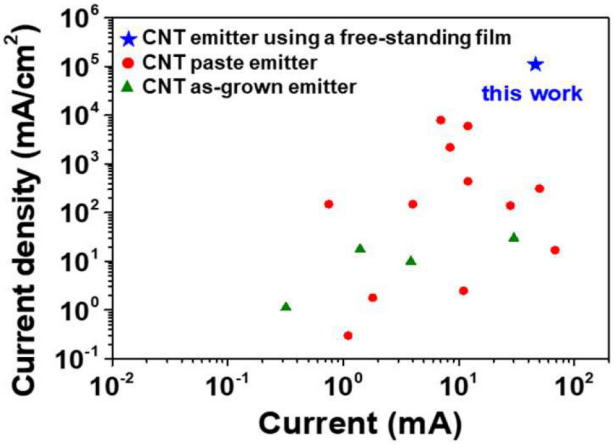


**FIGURE 6. Comparison of the emission current density according to CNT field emitters.**

electron beam reaching the phosphor screen through the gate electrode had a rectangular shape with a size of 10 mm along the length direction (x-axis) and 14.9 mm along the thickness direction (y-axis). The size of the electron beam was larger in the thickness direction. This is attributed to the bending of the equipotential line applied to the microscopic region at the end of the film along the thickness direction (y-axis) is very strong as shown in Fig. 3(b). Therefore, the electron beam spreads more in the thickness direction. Fig. 5(b) shows the long-term emission stability of the CNT field emitter in the triode configuration. The measurements were performed for 15 h in the pulse operating mode. The peak cathode current is increased from 5.8 mA to 6.2 mA during the emission stability test. The increased emission current is caused by the electrical annealing effect of the emitter tip, which contributed to field electron emission [25]. The CNT field emitter indicates stable operation behavior without current degradation or deformation of the gate electrode. The good emission stability is primarily attributed to two factors. The first is the uniformly distributed electric field at the entire edge of the CNT film as shown in Fig. 3(a) and (c). The second is that no organic materials are used to fabricate the CNT field emitter using the free-standing film. The inset of Fig. 5(b) shows the current fluctuation rate of the emission current during the long-term emission stability of the CNT field emitter. The current fluctuation rate was calculated as the rate of change of current compared to the current at the previous time ($\Delta I/I \times 100(\%)$). The fluctuation range of the emission current was found to range between −2.9 and 2.8%, and the average fluctuation rate was approximately 0.66%. The obtained results indicate that the CNT field emitter has good emission stability without emission current degradation and small fluctuation in the pulse operating mode. Fig. 6 shows a comparison of the emission current density according to CNT field emitters [10], [11], [16], [19], [28], [29], [32]–[41]. To investigate the performance of the CNT field emitter exactly, we compared the emission current density of each CNT field emitter because CNT field emitters indicated a different emission area. The CNT field emitter using a free-standing CNT film exhibited a very high emission current density of 100 A/cm$^2$. On the other hand, CNT field emitters made by as-grown CNTs showed a low current density below 30 mA/cm$^2$ [10], [11], [40], [41] and the CNT field emitters made by CNT paste showed a current density below 10 A/cm$^2$ [16], [19], [28], [29], [32]–[39]. For cold cathode X-ray sources, it is necessary for CNT field emitters to have both the high emission current and the high emission current density. Therefore, our CNT field emitter using a free-standing CNT film can be considered to be very appropriate for cold cathode X-ray source applications compared with other CNT field emitters.

## IV. CONCLUSION

We fabricated a CNT field emitter with a line-shape using a free-standing CNT film and investigated its field emission characteristics. The CNT field emitter indicated both the high emission current and the high emission current density, which is important to several applications of field emission devices. The high emission current density of the CNT field emitter is particularly attributed to the high-density emission sites at the edge of the CNT film. In addition, the organic binder free fabrication process and a uniformly distributed electric field at the edge of the CNT film help increase the field emission stability. It is suggested that the CNT field emitter can be used for diverse applications such as X-ray sources, deep UV sources, and electron beam sources in the future.

## REFERENCES

[1] C. T. White and T. N. Todorov, "Carbon nanotubes as long ballistic conductors," *Nature*, vol. 393, no. 6682, pp. 240–242, May 1998, doi: 10.1038/30420.
[2] P. Kim, L. Shi, A. Majumdar, and P. L. McEuen, "Thermal transport measurements of individual multiwalled nanotubes," *Phys. Rev. Lett.*, vol. 87, no. 21, Oct. 2021, Art. no. 215502, doi: 10.1103/PhysRevLett.87.215502.
[3] M. M. J. Treacy, T. W. Ebbesen, and J. M. Gibson, "Exceptionally high young's modulus observed for individual carbon nanotubes," *Nature*, vol. 381, no. 6584, pp. 678–680, Jun. 1996, doi: 10.1038/381678a0.
[4] P. M. Ajayan, "Nanotubes from carbon," *Chem. Rev.*, vol. 99, no. 7, pp. 1787–1799, Jul. 1999, doi: 10.1021/cr970102g.
[5] Y. Saito, and S. Uemura, "Field emission from carbon nanotubes and its application to electron sources," *Carbon*, vol. 38, no. 2, pp. 169–182, 2000, doi: 10.1016/S0008-6223(99)00139-6.
[6] W.-S. Cho *et al.*, "Carbon nanotube-based triode field emission lamps using metal meshes with spacers," *IEEE Electron Device Lett.*, vol. 28, no. 5, pp. 386–388, May 2007, doi: 10.1109/led.2007.895435.
[7] K. B. K. Teo *et al.*, "Microwave devices—Carbon nanotubes as cold cathodes," *Nature*, vol. 437, no. 7061, p. 968, Oct. 2005, doi: 10.1038/437968a.
[8] J. Zhang *et al.*, "Stationary scanning x-ray source based on carbon nanotube field emitters," *Appl. Phys. Lett.*, vol. 86, no. 18, May 2005, Art. no. 184104, doi: 10.1063/1.1923750.
[9] S. Park *et al.*, "A fully closed nano-focus X-ray source with carbon nanotube field emitters," *IEEE Electron Device Lett.*, vol. 39, no. 12, pp. 1936–1939, Dec. 2018, doi: 10.1109/led.2018.2873727.
[10] C. J. Lee *et al.*, "Synthesis of aligned carbon nanotubes using thermal chemical vapor deposition," *Chem. Phys. Lett.*, vol. 312, nos. 5–6, pp. 461–468, Oct. 1999, doi: 10.1016/S0009-2614(99)01074-X.

[11] D. T. Li, Y. J. Cheng, Y. J. Wang, H. Z. Zhang, C. K. Dong, and D. Li, "Improved field emission properties of carbon nanotubes grown on stainless steel substrate and its application in ionization gauge," *Appl. Surf. Sci.*, vol. 365, pp. 10–18, Mar. 2016, doi: 10.1016/j.apsusc.2016.01.011.

[12] J. Lim *et al.*, "Design and fabrication of CNT-based *E*-gun using stripe-patterned alloy substrate for X-ray applications," *IEEE Trans Electron Devices*, vol. 66, no. 12, pp. 5301–5304, Dec. 2019, doi: 10.1109/ted.2019.2943870.

[13] S. J. Oh, J. Zhang, Y. Cheng, H. Shimoda, and O. Zhou, "Liquid-phase fabrication of patterned carbon nanotube field emission cathodes," *Appl. Phys. Lett.*, vol. 84, no. 19, pp. 3738–3740, May 2004, doi: 10.1063/1.1737074.

[14] S. I. Jung, J. S. Choi, H. C. Shim, S. Kim, S. H. Jo, and C. J. Lee, "Fabrication of probe-typed carbon nanotube point emitters," *Appl. Phys. Lett.*, vol. 89, no. 23, Dec. 2006, Art. no. 233108, doi: 10.1063/1.2402222.

[15] W. B. Choi *et al.*, "Fully sealed, high-brightness carbon-nanotube field-emission display," *Appl. Phys. Lett.*, vol. 75, no. 20, pp. 3129–3131, Nov. 1999, doi: 10.1063/1.125253.

[16] J. H. Kim *et al.*, "Effect of micro and nanoparticle inorganic fillers on the field emission characteristics of photosensitive carbon nanotube pastes," *Appl. Surf. Sci.*, vol. 256, no. 8, pp. 2636–2642, Feb. 2010, doi: 10.1016/j.apsusc.2009.11.010.

[17] Y. C. Kim *et al.*, "Uniform and stable field emission from printed carbon nanotubes through oxygen trimming," *Appl. Phys. Lett.*, vol. 92, no. 26, Jun. 2008, Art. no. 263112, doi: 10.1063/1.2952771.

[18] Y. Sun *et al.*, "Fabrication of carbon nanotube emitters on the graphite rod and their high field emission performance," *Appl. Phys. Lett.*, vol. 104, no. 4, Jan. 2014, Art. no. 43104, doi: 10.1063/1.4863415.

[19] J.-W. Kim, J.-W. Jeong, J.-T. Kang, S. Choi, S. Ahn, and Y.-H. Song, "Highly reliable field electron emitters produced from reproducible damage-free carbon nanotube composite pastes with optimal inorganic fillers," *Nanotechnology*, vol. 25, no. 6, Feb. 2014, Art. no. 65201, doi: 10.1088/0957-4484/25/6/065201.

[20] Y. Wei, K. Jiang, L. Liu, Z. Chen, and S. Fan, "Vacuum-breakdown-induced needle-shaped ends of multiwalled carbon nanotube yarns and their field emission applications," *Nano Lett.*, vol. 7, no. 12, pp. 3792–3797, Dec. 2007, doi: 10.1021/nl072298y.

[21] G. Chen, D. H. Shin, S. Roth, and C. J. Lee, "Field emission characteristics of point emitters fabricated by a multiwalled carbon nanotube yarn," *Nanotechnology*, vol. 20, no. 31, Aug. 2009, Art. no. 315201, doi: 10.1088/0957-4484/20/31/315201.

[22] W.-J. Zhao, A. Sawada, and M. Takai, "Field emission characteristics of screen-printed carbon nanotube after laser irradiation," *Jpn. J. Appl. Phys.*, vol. 41, no. 6S, pp. 4314–4316, Jun. 2002, doi: 10.1143/jjap.41.4314.

[23] D.-H. Kim, C.-D. Kim, and H. R. Lee, "Effects of the ion irradiation of screen-printed carbon nanotubes for use in field emission display applications," *Carbon*, vol. 42, nos. 8–9, pp. 1807–1812, 2004, doi: 10.1016/j.carbon.2004.03.015.

[24] J. S. Lee, H. J. Lee, J. M. Yoo, T. Kim, and Y. H. Kim, "High-performance field emission from a carbonized cork," *ACS Appl. Mater. Interfaces*, vol. 9, no. 50, pp. 43959–43965, Dec. 2017, doi: 10.1021/acsami.7b11873.

[25] D. H. Shin *et al.*, "High performance field emission of carbon nanotube film emitters with a triangular shape," *Carbon*, vol. 89, pp. 404–410, Aug. 2015, doi: 10.1016/j.carbon.2015.03.041.

[26] L. Nilsson *et al.*, "Scanning field emission from patterned carbon nanotube films," *Appl. Phys. Lett.*, vol. 76, no. 15, pp. 2071–2073, Apr. 2000, doi: 10.1063/1.126258.

[27] G. S. Bocharov and A. V. Eletskii, "Effect of screening on the emissivity of field electron emitters based on carbon nanotubes," *Tech. Phys.*, vol. 50, no. 7, pp. 944–947, 2005, doi: 10.1134/1.1994978.

[28] K. Yoshihara, S. Fujii, H. Kawai, K. Ishida, S.-I. Honda, and M. Katayama, "Fabrication of screen-printed field electron emitter using length-controlled and purification-free carbon nanotubes," *Appl. Phys. Lett.*, vol. 91, no. 11, Sep. 2007, Art. no. 113109, doi: 10.1063/1.2784194.

[29] Y. Sun, K. N. Yun, G. Leti, S. H. Lee, Y.-H. Song, and C. J. Lee, "High-performance field emission of carbon nanotube paste emitters fabricated using graphite nanopowder filler," *Nanotechnology*, vol. 28, no. 6, Feb. 2017, Art. no. 65201, doi: 10.1088/1361-6528/aa523e.

[30] A. A. Al-Tabbakh, M. A. More, D. S. Joag, I. S. Mulla, and V. K. Pillai, "The Fowler–Nordheim plot behavior and mechanism of field electron emission from ZnO tetrapod structures," *ACS Nano*, vol. 4, no. 10, pp. 5585–5590, Oct. 2010, doi: 10.1021/nn1008403.

[31] M. Shiraishi and M. Ata, "Work function of carbon nanotubes," *Carbon*, vol. 39, no. 12, pp. 1913–1917, 2001, doi: 10.1016/s0008-6223(00)00322-5.

[32] G. Z. Yue *et al.*, "Generation of continuous and pulsed diagnostic imaging x-ray radiation using a carbon-nanotube-based field-emission cathode," *Appl. Phys. Lett.*, vol. 81, no. 2, pp. 355–357, Jul. 2002, doi: 10.1063/1.1492305.

[33] X. Calderón-Colón, H. Z. Geng, B. Gao, L. An, G. H. Cao, and O. Zhou, "A carbon nanotube field emission cathode with high current density and long-term stability," *Nanotechnology*, vol. 20, no. 32, Aug. 2009, Art. no. 325707, doi: 10.1088/0957-4484/20/32/325707.

[34] J. Yu, "Preparation of the printed carbon nanotubes cold cathode in field emission display and post-treatment technique using reactive ion etching," *Jpn. J. Appl. Phys.*, vol. 52, no. 2, Feb. 2013, Art. no. 25002, doi: 10.7567/jjap.52.025002.

[35] J.-W. Jeong, J.-W. Kim, J.-T. Kang, S. Choi, S. Ahn, and Y.-H. Song, "A vacuum-sealed compact x-ray tube based on focused carbon nanotube field-emission electrons," *Nanotechnology*, vol. 24, no. 8, Mar. 2013, Art. no. 85201, doi: 10.1088/0957-4484/24/8/085201.

[36] J.-W. Kim *et al.*, "Great improvement in adhesion and uniformity of carbon nanotube field emitters through reactive nanometer-scale SiC fillers," *Carbon*, vol. 82, pp. 245–253, Feb. 2015, doi: 10.1016/j.carbon.2014.10.068.

[37] H. R. Lee, S. W. Lee, C. Shikili, J. S. Kang, J. Lee, and K. C. Park, "Enhanced electron emission of paste CNT emitters with nickel buffer layer and its X-ray application," *J. Nanosci*, vol. 16, no. 11, pp. 12053–12058, Nov. 2016, doi: 10.1166/jnn.2016.13643.

[38] E. Go *et al.*, "Enhanced interfacial reaction of silicon carbide fillers onto the metal substrate in carbon nanotube paste for reliable field electron emitters," *Nanotechnology*, vol. 32, no. 19, May 2021, Art. no. 190001, doi: 10.1088/1361-6528/abe1ef.

[39] R. Jiang, J. Liu, K. Yang, J. Zhao, and B. Zeng, "Enhanced field emission of single-wall carbon nanotube cathode prepared by screen printing with a silver paste buffer layer," *Nanomaterials*, vol. 12, no. 1, p. 165, Jan. 2022, doi: 10.3390/nano12010165.

[40] A. Pandey, A. Prasad, J. P. Moscatello, M. Engelhard, C. M. Wang, and Y. K. Yap, "Very stable electron field emission from strontium titanate coated carbon nanotube matrices with low emission thresholds," *ACS Nano*, vol. 7, no. 1, pp. 117–125, Jan. 2013, doi: 10.1021/nn303351g.

[41] K.-Y. Wang, C.-Y. Liao, and H.-C. Cheng, "Field-emission characteristics of the densified carbon nanotube pillars array," *ECS J. Solid-State Sci. Technol.*, vol. 5, no. 9, pp. M99–M103, 2016, doi: 10.1149/2.0301609jss.